Published in final edited form as:
J Immunol. 2013 November 1; 191(9): . doi:10.4049/jimmunol.1300581.

Identification of a tissue-specific, C/EBPβ-dependent pathway of differentiation for murine peritoneal macrophages

Derek W. Cain[*], **Emily G. O'Koren**[*], **Matthew J. Kan**[*], **Mandy Womble**[*], **Gregory D. Sempowski**[*,†], **Kristen Hopper**[*], **Michael D. Gunn**[*,‡], and **Garnett Kelsoe**[*]

[*]Department of Immunology, Duke University, Durham, NC 27710

[†]Duke Human Vaccine Institute, Duke University, Durham, NC 27710

[‡]Department of Medicine, Duke University, Durham, NC 27710

Abstract

Macrophages and dendritic cells (DC) are distributed throughout the body and play important roles in pathogen detection and tissue homeostasis. In tissues, resident macrophages exhibit distinct phenotypes and activities, yet the transcriptional pathways that specify tissue-specific macrophages are largely unknown. We investigated the functions and origins of two peritoneal macrophage populations in mice, small- and large peritoneal macrophages (SPM and LPM, respectively). SPM and LPM differ in ability to phagocytose apoptotic cells and in the production of cytokines in response to LPS. In steady-state conditions, SPM are sustained by circulating precursors whereas LPM are maintained independently of hematopoiesis; both populations, however, are replenished by bone marrow (BM) precursors following radiation injury. Transcription factor analysis revealed that SPM and LPM express abundant CCAAT/enhancer binding protein (C/EBP)-β. C/EBPβ$^{-/-}$ mice exhibit elevated numbers of SPM-like cells but lack functional LPM. Alveolar macrophages are also missing in C/EBPβ$^{-/-}$ mice, although macrophage populations in the spleen, kidney, skin, mesenteric lymph nodes, and liver are normal. Adoptive transfer of SPM into C/EBPβ$^{-/-}$ mice results in SPM differentiation into LPM yet donor SPM do not generate LPM after transfer into C/EBPβ-sufficient mice, suggesting that endogenous LPM inhibit differentiation by SPM. We conclude that C/EBPβ plays an intrinsic, tissue-restricted role in the generation of resident macrophages.

Introduction

Animal tissues contain macrophages and DC that constitute a network of cells dubbed the mononuclear phagocyte system (1). Among tissues, resident phagocytes exhibit substantial phenotypic heterogeneity, likely reflecting tissue-specific function (2). Macrophage

Corresponding Author: Garnett Kelsoe DUMC Box 3010 Durham, NC 27710 Telephone: (919) 613-7815 Fax: (919) 613-7878 ghkelsoe@duke.edu.

Authorship Contributions

D.W.C.: Designed, conducted, and evaluated experiments and wrote the manuscript.
E.G.O.: Designed, conducted, and evaluated experiments.
M.J.K: Designed, conducted, and evaluated experiments.
M.W.: Designed, conducted, and evaluated experiments.
G.D.S.: Designed and evaluated experiments.
K.H.: Designed, conducted, and evaluated experiments.
M.D.G.: Designed and evaluated experiments.
G.K.: Designed and evaluated experiments, and wrote the manuscript.

Disclosure of Conflicts of Interest

The authors have no competing financial interests.

diversity is thought to result from environmental cues in tissues that induce distinct differentiation programs in macrophages or their precursors. However, the differentiation pathways that generate tissue-specific macrophages are largely unknown (3). Moreover, recent studies have challenged the long-standing hypothesis that tissue-resident macrophages arise from circulating monocytes (1), instead indicating that some macrophage compartments are established by fetal precursors and maintained independent of hematopoiesis (4, 5).

Macrophages of the murine peritoneal cavity are among the best studied tissue macrophage compartments. Peritoneal macrophages play important roles in clearing apoptotic cells (6) and coordinating inflammatory responses (7–9). A recent study demonstrated that mouse peritoneal macrophages can be divided into two subsets, large-and small peritoneal macrophages (LPM and SPM, respectively) (10). LPM comprise the majority of peritoneal macrophages and express high levels of F4/80, CD11b, and CD93 but lack MHCII; SPM, in contrast, express lower levels of F4/80, CD11b, and CD93 but high levels of MHCII (10). Both SPM and LPM phagocytose bacteria and produce NO (10), but little else is known of their origins and independent functions.

Studies in gene knockout mice have identified transcription factors that operate at discrete stages of macrophage differentiation. PU.1 and C/EBPα are necessary for the generation of macrophage precursors, as mice deficient for these transcription factors lack myeloid progenitors in BM and macrophages in various tissues (11, 12). In contrast, Spi-$C^{-/-}$ mice have normal myelopoiesis and macrophages in several tissues, but lack red pulp macrophages in the spleen (13). These observations indicate that distinct transcriptional pathways direct the differentiation of tissue-specific macrophages. A transcriptional pathway that specifies the generation of peritoneal macrophages has not been described.

In this study, we investigated the functions and origins of SPM and LPM; SPM and LPM diverged in their ability to phagocytose apoptotic cells and exhibited differences in cytokine production after LPS exposure. Transcription factor analysis revealed C/EBPβ expression by both SPM and LPM but in C/EBP$\beta^{-/-}$ mice, the peritoneal cavity lacked LPM while elevated numbers of SPM-like cells were present. We identify SPM as precursors of LPM, and show that C/EBPβ acts intrinsically in the differentiation or survival of LPM. Finally, adoptively transferred SPM efficiently generated LPM in C/EBP$\beta^{-/-}$ mice, but did not differentiate in normal mice in the presence of endogenous LPM. We interpret this suppression of differentiation as evidence of a demand-driven process for the replenishment of peritoneal macrophages from hematopoietic precursors.

Materials and Methods

Mice

C57BL/6 and congenic $LysM^{Cre/WT}$ and $CX_3CR1^{GFP/WT}$ mice came from The Jackson Laboratory. C/EBP$\beta^{+/-}$ mice on 129/Sv and C57BL/6 backgrounds were kindly provided by Dr. P. Johnson (NCI);129/Sv x C57BL/6.F1 C/EBP$\beta^{-/-}$ mice and control subjects were generated from hemizygous parents (14). 129/Sv x C57BL/6.eGFP^{+}.F1 mice were used as a source of peritoneal macrophages in adoptive transfer experiments. Transgenic mice expressing Cre recombinase under the regulatory elements of the CX_3CR1 gene (CX_3CR1^{Cre} mice, manuscript in preparation) were obtained from the Gene Expression Nervous System Atlas Project (15). C/EBP$\beta^{fl/fl}$ mice (16) were generously provided by Dr. E. Sterneck (NCI) and crossed with $LysM^{Cre/WT}$ mice to generate $LysM^{Cre/WT}$C/EBP$\beta^{fl/fl}$ and $LysM^{WT/WT}$C/EBP$\beta^{fl/fl}$ mice. Rosa26R- farnesylated GFP (FGFP) (17) mice were obtained from Dr. B. Hogan (Duke University) and crossed with $LysM^{Cre/WT}$ or CX_3CR1^{Cre} mice to generate $LysM^{Cre/WT}$Rosa26R-FGFP and $LysM^{WT/WT}$Rosa26R-FGFP mice, and

$CX_3CR1^{Cre/WT}$Rosa26R-FGFP and $CX_3CR1^{WT/WT}$Rosa26R-FGFP mice, respectively. Mice were housed in a specific pathogen-free facility and provided with sterilized chow and water *ad libitum*. All procedures were approved by the Duke University Institutional Animal Care and Use committee.

Flow cytometry

FITC-, Alexa Fluor 488-, PE-, PE-Cy5-, APC-, APC-eFluor780-, PE-Texas Red-, PE-Cy7, and biotinylated antibodies to F4/80, SIGN-R1, MOMA-1, CD11c, CD93, CD11b, MHCII (I-A/I-E), TCRβ, B220, Gr-1, Ly-6B, Siglec F, CD115, CD205, and IgM were obtained from eBioscience, BD Biosciences, or AbD Serotec.

Peritoneal cells were harvested by lavage with 7 ml cold PBS. Blood was harvested with a heparinized 27G needle from the inferior vena cava. Mice were perfused with PBS and lung, liver, mesenteric lymph nodes, spleen, kidneys, and ears were harvested. Organs were manually dissociated and digested for 1 hour at 37°C with 2 mg/mL collagenase A (Roche Applied Science) and 0.2 mg/mL DNase I (Roche Applied Science) in 5% FBS with 10 mM HEPES. Cells were strained through a 70 um filter and washed with PBS. For the liver and kidney, cells were centrifuged in a 30% over 70% Percoll (Invitrogen) in PBS density gradient. Interface cells were isolated and RBC lysed with ACK buffer.

Cells were stained with optimal concentrations of fluorochrome-antibody conjugates. Biotinylated antibodies were detected with streptavidin-fluorochrome conjugates. For detection of intracellular C/EBPβ protein, cells were fixed and permeabilized (eBioscience fixation/permeabilization buffers) before incubation with anti-C/EBPβ or rabbit IgG isotype control (Santa Cruz Biotechnology); primary antibodies were detected with PE-conjugated anti-rabbit IgG (SouthernBiotech).

Labeled cells were analyzed on a LSRII flow cytometer (BD Biosciences) or sorted on a FACS Aria (BD Biosciences). Propidium iodide (Sigma) or Live/Dead Aqua (Invitrogen) staining excluded dead cells. Data were analyzed with Flow Jo software (Treestar).

Quantitative RT-PCR

Peritoneal B cells, DC, SPM, and LPM were purified by FACS. RNA was harvested using a Nanoprep RNA kit (Agilent Technologies) and cDNA generated with SuperScript III reagents (Invitrogen) and oligo-dT primers. Gene transcription was determined using SsoFast EvaGreen reagents (Bio-Rad) and the following primers: GAPDH, forward 5'-AAC TTT GGC ATT GTG GAA GG-3' and reverse 5'-ACA CAT TGG GGG TAG GAA CA-3'; β-actin, forward 5'-AGC CAT GTA CGT AGC CAT CC-3' and reverse 5'- CTC TCA GCT GTG GTG GTG AA-3'; C/EBPβ, forward 5'- AAG CTG AGC GAC GAG TAC AAG A-3' and reverse 5'-GTC AGC TCC AGC ACC TTG TG-3'. cDNA was amplified in a CFX96 Real-Time System (Bio-Rad) with the following parameters: 95°C, 30 sec; 40 cycles of 95°C for 5 sec, 60°C for 10 sec. Relative gene expression was calculated by the comparative CT (threshold cycle) normalized to β-actin message; ΔCT values were determined by subtracting CT (target) from CT (β-actin). Expression levels relative to β-actin were defined as $2^{-\Delta CT}$. Average expression levels of GAPDH and C/EBPβ in the peritoneal DC compartment were set as 1; expression levels in other compartments were normalized to this value.

Cytokine induction by LPS

Peritoneal DC, SPM, and LPM were isolated by FACS then suspended at 10^5 cells/ml in RPMI-1640 medium containing 10% FBS, 10 mM HEPES, 55 μM 2-ME, and penicillin/

streptomycin. Cells were treated or not with 1 μg/ml LPS (O127:B8, Sigma-Aldrich) overnight at 37°C/5% CO_2; supernatants were stored at −80°C.

Phagocytosis of apoptotic cells

Phagocytic activity was assayed as previously described (18). Briefly, syngeneic thymocytes (10^7 cells/ml) were cultured with 0.1 μM dexamethasone overnight to induce apoptosis. The frequency of Annexin V^+ cells was 65–85%. Apoptotic thymocytes (10^6 cells/ml) were incubated with 0.02 μg/ml pHrodo™ Red (Invitrogen) for 30 min, washed in PBS, and then injected *i.p.* (10^6 cells per mouse). One hour later, mice were sacrificed and the peritoneal cavity lavaged for flow cytometric analysis.

BrdU uptake analysis

Mice were injected *i.p.* with 1 mg BrdU in 200 μl PBS and sacrificed at various intervals. BrdU incorporation was determined in cell compartments using a BrdU detection kit (BD Biosciences). Peritoneal lavage and BM cells were stained for surface antigens with fluorochrome-antibody conjugates, fixed/permeabilized, treated with DNase, and stained with FITC anti-BrdU. Frequencies of $BrdU^+$ SPM and LPM were determined by flow cytometry, using corresponding cell populations from untreated mice as background controls.

Histology and immunofluorescence

Tissues were frozen in OCT compound. Sections (5 μm) were fixed in methanol/acetone (1:1) and blocked with rat IgG and Fc block. Sequential sections were stained with FITC MOMA-1, PE F4/80, and biotin B220, or AlexaFluor488 SIGN-R1, PE TCRβ, and biotin B220. Biotin mAb were detected with Streptavidin AlexaFluor350. Images were acquired at room temperature using a Zeiss Axiovert 200M microscope with 10× objective lens (0.30 numerical aperture), Zeiss AxioCam MRm camera, and Axiovision software. Composite micrographs were generated in Adobe Photoshop using B220 labeling to align images from sequential sections.

Quantification of cytokines in culture supernatants and sera

Soluble cytokines were analyzed in the Duke Human Vaccine Institute Immune Reconstitution & Biomarker Shared Resource Facility. Supernatants from untreated and LPS-treated DC, SPM, and LPM were analyzed. Sera were prepared from C/EBP$\beta^{+/+}$ and C/EBP$\beta^{-/-}$ mice. Cytokine concentrations in samples were determined using a Bio-Plex Pro Group I 23-Plex kit (Bio-Rad).

Adoptive transfer of peritoneal macrophages

Peritoneal cells of 129/Sv x C57BL/6.eGFP$^+$.F1 mice were stained with fluorochrome-antibody conjugates. SPM were identified as $B220^-IgM^-CD4^-CD8^-CD11c^-F4/80^{low}CD11b^+$ and LPM as $B220^-IgMCD4^-CD8^-CD11c^-F4/80^{hi}CD11b^+$. Sorted cells ($8\times10^4$) were injected *i.p.* into C/EBPβ-sufficient (C/EBP$\beta^{+/+}$ or C/EBP$\beta^{+/-}$) or C/EBP$\beta^{-/-}$ mice; recipient mice were sacrificed and peritoneal lavages analyzed on days 2, 4, 8, and 30 after transfer.

Adoptive reconstitution

C57BL/6 mice were sublethally irradiated (600 rad) and reconstituted with 10^7 BM cells from congenic C57BL/6.CD45.1 mice. Peritoneal cells of chimeric mice were analyzed 4–5 weeks after reconstitution; donor-derived cells were distinguished by CD45.1 expression.

Statistics

Significance in paired data was determined by Student's t-test. Significance in multiple comparisons was determined by ANOVA with Tukey post-hoc test (JMP Pro).

Results

Characterization of peritoneal macrophages and dendritic cells

Peritoneal lavage cells from naive C57BL/6 mice were analyzed by flow cytometry and IgM^+SSC^{low} B cells were excluded for analysis of myeloid cells (Fig. 1A). We identified a population of $IgM^-CD11c^+SSC^{low}$ cells that were uniformly $MHCII^+CD93^-$ and exhibited a broad distribution of CD115, the M-CSF receptor (Fig. 1A). Most (75–90%) $IgM^-CD11c^+SSC^{low}$ cells were $CD11b^+$ (Fig. 1A), consistent with the "myeloid" DC phenotype of lymphoid tissues, whereas the remaining $CD11b^-$ cells expressed CD205, similar to "lymphoid" DC (19) (Fig. 1A). Hereafter, we refer to $IgM^-CD11c^+SSC^{low}$ cells collectively as DC.

Within the IgM^-CD11c^{low} cell population, we observed two $CD11b^+$ populations with high side-scatter properties that could be distinguished by intermediate and high levels of CD11b (Fig. 1A). $CD11b^{int}SSC^{hi}$ cells were $CD115^{low}$Siglec F^+ and identified as eosinophils by histological analysis (data not shown). The $CD11b^{hi}SSC^{hi}$ compartment was further sub-divided by F4/80 staining; the $F4/80^{low}$ cells, comprising <5% of $CD11b^{hi}SSC^{hi}$ cells, exhibited greater light scattering than DC and were $CD115^+MHCII^{hi}CD93^-CD205^{low}$ (Fig. 1A), consistent with the SPM phenotype (10). The $F4/80^{hi}$ cells exhibited higher side-scatter properties than SPM and were $CD115^+MHCII^{low}CD93^+CD205^-$ (Fig. 1A), consistent with the LPM phenotype (10).

To characterize the functions of peritoneal DC, SPM, and LPM, cells were isolated by FACS and then analyzed for cytokine production in response to LPS *in vitro*. LPS stimulated all three cell types to secrete IL-1β, IL-9, IL-12(p70), IL-13, eotaxin, and IFNγ, and there were only modest differences (<2-fold) across the three cell compartments (Fig. 1B, Supplemental Fig. 1). SPM, however, produced significantly more MIP-1α and TNFα than either DC or LPM (Fig. 1B, Supplemental Fig. 1). LPM, in contrast, selectively produced abundant G-CSF, GM-CSF, and KC in response to LPS whereas DC exclusively generated IL-12(p40) (Fig. 1B, Supplemental Fig. 1). DC and SPM were more potent sources of RANTES than LPM, but SPM and LPM produced significantly more IL-1α, IL-6, IL-10, MCP-1, and MIP-1β than DC (Fig. 1B, Supplemental Fig. 1). The discrete cytokine profiles of LPS-treated DC, SPM, and LPM suggest that these myeloid compartments contribute differently to inflammatory responses in the peritoneal cavity.

Resident phagocytes contribute to tissue homeostasis by clearing dying cells (6); consequently, we measured the capacity of peritoneal DC, SPM, and LPM to phagocytose apoptotic cells. Apoptotic thymocytes were labeled with pHrodo Red, a dye that fluoresces at increased intensity following transport into acidic lysosomes (18), and then injected *i.p.* into mice. After one hour, mice were sacrificed and peritoneal cells analyzed by FACS for the presence of pHrodo Red. Frequencies of pHrodo Red^+ cells in each macrophage compartment varied among mice, but in all animals the frequency of labeled LPM was greater than SPM (Fig. 1C). The ratio of labeled LPM to SPM was 3.8±1.3 (geometric mean ±GSD, range 2.9–4.9), indicating that LPM exhibit greater phagocytic activity than SPM. The frequency of labeled DC was only slightly higher than background whereas eosinophils lacked label (Fig. 1C). While both SPM and LPM have the capacity to engulf apoptotic cells, LPM are the more potent phagocytes.

Origins and maintenance of the peritoneal DC, SPM, and LPM compartments

The mononuclear phagocyte system is thought to depend on hematopoiesis for the maintenance of tissue phagocytes, with circulating monocytes serving as cellular intermediates between BM progenitors and tissue-resident macrophages (1). However, reports of *in situ* proliferation suggest that some macrophage compartments have the capacity for self-replenishment (20). To quantify *in situ* proliferation by peritoneal DC, SPM and LPM, we measured frequencies of BrdU-labeled cells in these myeloid compartments three hours after BrdU administration. The frequencies of $BrdU^+$ DC, SPM, and LPM were 0.7%, 1.2%, and 2.4%, respectively, whereas autologous frequencies of $BrdU^+$ BM hematopoietic stem cell ($Lin^-Sca\text{-}1^+c\text{-}Kit^+Flt3^-$) and granulocyte/macrophage progenitor ($Lin^-Sca\text{-}1^-c\text{-}Kit^+CD16/32^+$) compartments were 18% and 39%, respectively (Fig. 2A). Peritoneal DC, SPM, and LPM undergo little proliferation in the steady-state.

We next monitored the appearance of BrdU label in peritoneal myeloid compartments after BrdU injection as an indication of differentiation from proliferating precursors. The frequency of $BrdU^+$ DC and SPM increased after BrdU administration, peaking at days 4–6 and 6–10, respectively, before gradually returning to background levels (Fig. 2B). DC and SPM acquired BrdU label regardless of BrdU injection route (day 6 *i.p.* vs. *i.v.*: 17.7% *vs.* 17.2% for DC, 5.8% *vs.* 5.4% for SPM, P>0.05 all), indicating that the appearance of BrdU label in these populations after *i.p.* injection was not due to local inflammation. We conclude that peritoneal DC and SPM are continuously produced from proliferating precursors and have tissue half-lives of only a few days.

In contrast to DC and SPM, BrdU labeling was not detectable in the LPM compartment over 14 days after the BrdU pulse (Fig. 2B), suggesting that LPM, in steady-state conditions, are long-lived and/or sustained by a low level of proliferation *in situ*. This observation is consistent with previous studies showing that $F4/80^{hi}$ peritoneal macrophages (LPM) persist independently of BM hematopoiesis (21, 22).

To investigate the relationships between peritoneal phagocytes and myeloid precursors, we analyzed peritoneal DC, SPM, and LPM from $CX_3CR1^{GFP/WT}$ mice, in which GFP reports transcription of CX_3CR1, a chemokine receptor expressed by macrophage/dendritic cell progenitors and monocytes (23). In $CX_3CR1^{GFP/WT}$ mice, DC were almost uniformly GFP^+ whereas SPM exhibited a broad distribution of GFP; LPM, however, were GFP^- (Fig 2C). In contrast, in CX_3CR1^{Cre}Rosa26R-FGFP mice which identify both active and past expression of CX_3CR1, ~90% of DC and nearly all SPM and LPM were GFP^+ (Fig. 2C). We conclude that most peritoneal DC and all SPM are short-lived, recent descendants of CX_3CR1^+ precursors, whereas LPM exhibit a more distant ontogenic relationship with a CX_3CR1^+ progenitor.

Although macrophages are commonly thought to differentiate from circulating monocytes (1), recent reports indicate that some tissue-resident macrophages arise from CX_3CR1^+ precursors in the yolk sac and are maintained independent of hematopoietic stem cells (4, 5). To determine the relationship between BM hematopoiesis and peritoneal DC, SPM, and LPM, we irradiated C57BL/6 mice and reconstituted with C57BL/6.CD45.1 BM. Four weeks after BM reconstitution, ~90% of peritoneal DC and ~80% of SPM were $CD45.1^+$, indicative of hematopoietic origin. Although previous studies (21, 22) and our BrdU transit study (Fig. 2B) indicate that the LPM compartment is maintained independent of hematopoiesis in the steady-state, greater than 70% of LPM in chimeric mice were $CD45.1^+$ (Fig. 2D), demonstrating a pathway of differentiation from BM precursors to LPM. We conclude that in steady-state conditions, the peritoneal DC and SPM compartments are sustained through hematopoiesis whereas LPM are maintained independently of BM. The

cytotoxic effects of radiation, however, activate a pathway of hematopoietic differentiation that replenishes the LPM compartment.

Altered phenotype and function of peritoneal macrophages in C/EBPβ$^{-/-}$ mice

Studies in Spi-C$^{-/-}$ mice highlight the specificity of transcription factors for the generation of distinct tissue macrophage compartments (13). In addition to *Spi-c*, transcription factors implicated in macrophage differentiation include *C/EBP*β (24), *Egr1* (25), *Irf5 (26), Maf (27), Mafb (27), Mitf (28),* and *Nfya* (29). Micro-array analysis of transcription factor expression by tissue macrophages revealed that C/EBPβ is highly expressed in peritoneal macrophages (F4/80^{hi}CD115^{+}B220^{-}MHCII^{-} cells, consistent with the LPM phenotype) (30). Using quantitative RT-PCR, we confirmed that C/EBPβ transcription was high in LPM, whereas levels were intermediate in SPM, low in peritoneal DC, and undetectable in B cells (Fig. 3A). Similar results were obtained from analysis of C/EBPβ protein levels by flow cytometry (Fig. 3B).

We next investigated peritoneal macrophages in C/EBPβ$^{-/-}$ mice. Viability of C/EBPβ$^{-/-}$ pups with the C57BL/6 genetic background is low (31), therefore we produced C/EBPβ$^{-/-}$ mice by crossing heterozygous C57BL/6 and 129/Sv parents, generating C57BL/6x129/Sv.F1 C/EBPβ$^{-/-}$ mice and control littermates at expected Mendelian ratios (14). Peritoneal macrophage compartments were comparable in numbers and phenotype in C57BL/6 and C57BL/6x129/Sv.F1 C/EBPβ$^{+/+}$ mice (data not shown).

C/EBPβ deficiency severely affected peritoneal macrophage compartments. In C/EBPβ$^{-/-}$ mice, the overall number of peritoneal macrophages (IgM^{-}CD11c^{-}CD11b^{hi} cells) was only 35% of that in C/EBPβ$^{+/+}$ mice (P≤0.01) (Fig. 3B and C). Whereas F4/80 labeling revealed SPM and LPM as discrete populations in C/EBPβ$^{+/+}$ and C/EBPβ$^{+/-}$mice, distinct F4/80^{hi} and F4/80^{low} macrophage populations were not found in C/EBPβ$^{-/-}$ mice (Fig. 3B). Instead, we noted a homogenous population of cells exhibiting low to intermediate levels of F4/80 (F4/80^{low} and F4/80^{int}, respectively), with <10% of cells falling into the F4/80^{hi} gate (Fig. 3B). Compared to control littermates, the numbers of F4/80^{low} and F4/80^{int} peritoneal macrophages in C/EBPβ$^{-/-}$ mice were increased 6- and 25-fold, respectively (P≤0.01), whereas the number of F4/80^{hi} macrophages was reduced >95% (P≤0.01) (Fig. 3B, C). In C/EBPβ$^{-/-}$ mice, peritoneal DC numbers were modestly, but not significantly, increased (Fig. 3C) whereas the number of CD11b^{int}SSC^{hi} cells, identified as eosinophils, was elevated 10-fold over controls (Supplemental Fig. 3A).

We analyzed C/EBPβ$^{-/-}$macrophages for MHCII and CD93, markers that distinguish SPM and LPM in control animals. Peritoneal macrophages of C/EBPβ$^{-/-}$ mice were dividable by MHCII staining into a F4/80^{low}MHCII^{hi} compartment (similar to SPM in control mice), a F4/80^{int}MHCII^{int} population, and a F4/80^{int} population exhibiting levels of MHCII that were low and similar to LPM in C/EBPβ$^{+/+}$ animals (Fig. 3E). The frequency of F4/80^{low}MHCII^{hi} SPM-like cells was 4–5 fold higher in C/EBPβ$^{-/-}$ mice than control animals, with a concurrent reduction in frequency of F4/80^{int}MHCII^{low} LPM-like cells (Fig. 3E). Unlike wild-type LPM, however, F4/80^{int} macrophages in C/EBPβ$^{-/-}$ mice did not express CD93 (Fig. 3E). Moreover, C/EBPβ$^{-/-}$ F4/80^{int} macrophages exhibited high levels of CD115 similar to a transitional population of cells in WT mice (Fig. 3E). Overall, C/EBPβ deficiency was associated with an increased number of peritoneal macrophages bearing the SPM phenotype (F4/80^{low}MHCII^{+}CD93^{-}CD115^{int}), a CD115^{hi} macrophage population sharing characteristics of both SPM (CD93^{-}) and LPM (MHCII$^{int\text{-}low}$), but no cells exhibiting the complete LPM phenotype (F4/80^{hi}MHCII^{low}CD93^{+}CD115$^{int\text{-}low}$).

The absence of F4/80^{hi}CD93^{+} macrophages in C/EBPβ$^{-/-}$ mice suggested a defect in LPM generation. Alternatively, LPM may be normal in C/EBPβ$^{-/-}$ mice but fail to express F4/80

and CD93 due to dysregulation of the corresponding genes. To determine if F4/80^{int}MHCII^{low} LPM-like cells in C/EBPβ$^{-/-}$ mice function as LPM, we compared the phagocytic activity of F4/80^{low}MHCII^{hi} SPM-like cells and F4/80^{int}MHCII^{low} LPM-like cells in C/EBPβ KO mice. Following injection of pHrodo Red labeled apoptotic cells, the ratio of labeled LPM to SPM was 3.5±1.3 (geometric mean±GSD; range = 2.6–5.0) in C/EBPβ$^{+/+}$ littermates, similar to that in BL/6 mice (Fig. 3F). In C/EBPβ$^{-/-}$ mice, however, the ratio of labeled F4/80^{int}MHCII^{low} LPM-like cells to F4/80^{low}MHCII^{hi} SPM-like cells mice was only 1.6±1.2 (range = 1.5–1.9) (P≤0.05 C/EBPβ$^{-/-}$ *vs.* C/EBPβ$^{+/+}$, BL/6). Based on phenotypic and functional analyses of C/EBPβ$^{-/-}$ peritoneal macrophages, we conclude that C/EBPβ is necessary for the generation of LPM.

C/EBPβ is induced by inflammatory stimuli and affects cytokine production in several macrophage types, including peptone-elicited macrophages (32), alveolar macrophages (33), splenic macrophages (34), and other subtypes (35, 36). Peritoneal macrophages of C/EBPβ KO also exhibited altered cytokine production. Overall, LPS-induced cytokine responses of SPM-like (IgM^{-}CD11c^{low}CD11b^{+}SSC^{hi}MHCII^{hi}) and LPM-like (IgM^{-}CD11c^{low}CD11b^{+}SSC^{hi}MHCII^{low}) cells from C/EBPβ$^{-/-}$ mice were decreased compared to WT SPM and LPM, respectively (Supplemental Fig. 2). In both SPM-like and LPM-like cells of C/EBPβ$^{-/-}$ mice, the cytokines most affected included IL-6, G-CSF, and MIP-1α Supplemental Fig. 2). However, both SPM- and LPM-like macrophages of KO mice produced more IL-12(p40) than corresponding WT cells, consistent with observations in other macrophage subtypes (35). MCP-1 secretion was also elevated in C/EBPβ$^{-/-}$ macrophages compared to control cells (Supplemental Fig. 2). As observed in other macrophages, C/EBPβ plays an integral role in the cytokine responses of peritoneal macrophages.

C/EBPβ deletion in LysM-expressing cells blocks LPM generation

C/EBPβ is expressed by many cell types (14, 31, 37); consequently, we determined if C/EBPβ acts intrinsically for LPM generation. LysM$^{Cre/WT}$ mice delete floxed alleles in granulocytes and macrophages (38). Using LysM$^{Cre/WT}$Rosa26R-FGFP mice, we confirmed that in the peritoneal cavity, Cre recombinase activity is primarily restricted to SPM and LPM, although ~35% of DC were also GFP^{+} (Fig. 4A).

The peritoneal phenotype of LysM$^{Cre/wt}$C/EBPβ$^{fl/fl}$ mice was similar to that of C/EBPβ$^{-/-}$ mice, despite differences in genetic background (C57BL/6 for LysM$^{Cre/wt}$C/EBPβ$^{fl/fl}$ mice; 129/SvxC57BL/6.F1 for C/EBPβ$^{-/-}$ mice) and general *vs.* conditional deletion of C/EBPβ. In LysM$^{Cre/wt}$C/EBPβ$^{fl/fl}$ mice, F4/80^{hi} LPM-like cell numbers were reduced >95% (P≤0.01) and F4/80^{low} SPM-like cell numbers were increased 7-fold (P≤0.01) compared to controls (Fig. 4B and C). As in C/EBPβ$^{-/-}$ mice, LysM$^{Cre/wt}$C/EBPβ$^{fl/fl}$ mice lacked peritoneal macrophages bearing the LPM phenotype of MHCII^{low}CD93^{+} (Fig. 4B). We conclude that C/EBPβ deficiency in macrophages is sufficient to prevent LPM generation.

Constitutive peritoneal eosinophilia in C/EBPβ$^{-/-}$ mice

While C/EBPβ$^{-/-}$ mice exhibited altered peritoneal macrophage populations, peritoneal B-cell numbers (1.3±1.0×10^{6}, 1.7±1.4×10^{6}, and 0.7±0.3×10^{6}) were not different in C/EBPβ$^{+/+}$, C/EBPβ$^{+/-}$, and C/EBPβ$^{-/-}$ mice (respectively; P>0.05, all). However, a population of CD11b^{int}SSC^{hi} cells was greatly expanded (>10-fold, P<0.05) (Supplemental Fig. 3A and B). Similar to C/EBPβ$^{-/-}$ mice, the number of CD11b^{int}SSC^{hi} cells was also significantly elevated in the peritoneal cavity of LysM$^{Cre/wt}$C/EBPβ$^{fl/fl}$ mice (Supplemental Fig. 3B). The CD11b^{int}SSC^{hi} cells were Siglec F^{hi}CD115^{lo} (Supplemental Fig. 3C) and, when isolated, exhibited eosinophil morphology (data not shown). The peritoneal eosinophilia of C/EBPβ$^{-/-}$ mice and LysM$^{Cre/wt}$C/EBPβ$^{fl/fl}$ mice was not associated with increased eosinophil

numbers in the BM or blood (Supplemental Fig. 3D), suggesting that their abundance in the peritoneal cavity is not due to enhanced eosinopoiesis.

The altered peritoneal macrophage and eosinophil populations raised the possibility that C/EBPβ deficiency might provoke inflammation; aged C/EBPβ$^{-/-}$ mice routinely develop an inflammatory pathology mediated by IL-6 (39). We examined the peritoneal lavages of C/EBPβ$^{-/-}$ mice for neutrophils and inflammatory monocytes (Gr-1^{+}Ly-6B^{+} cells) as evidence of local inflammation, but found neutrophil and inflammatory monocyte numbers to be similar in C/EBPβ$^{+/+}$ and C/EBPβ$^{-/-}$ mice (Supplemental Fig. 3E).

We next analyzed the sera of C/EBPβ$^{+/+}$ and C/EBPβ$^{-/-}$ mice for evidence of systemic inflammation. Multiplex analysis of sera did not reveal any differences in the concentrations of 23 cytokines, including IL-6 (Supplemental Fig. 3F). There was no evidence that altered macrophage and eosinophil populations in the peritoneal cavity of C/EBPβ$^{-/-}$ mice were due to ongoing inflammation.

C/EBPβ deficiency affects alveolar macrophages, but not macrophage populations in spleen, lymph node, liver, kidney, or skin

To determine if C/EBPβ plays a general role in macrophage generation, we analyzed C/EBPβ KO and littermate controls for blood monocytes and resident macrophages of the spleen, mesenteric lymph nodes, skin, kidneys, liver, and lungs. Frequencies of F4/80^{+}SSC^{low} monocytes in blood were similar in C/EBPβ$^{+/+}$ and C/EBPβ$^{-/-}$ mice, and all tissues from C/EBPβ$^{-/-}$ animals, with the exception of lung, contained similar frequencies of F4/80^{+} macrophages as controls (Fig. 5A). C/EBPβ is dispensable for the general production of cells in the monocyte/macrophage lineage.

In the lungs of C/EBPβ$^{-/-}$ mice, the frequency of F4/80^{+}CD11b^{low} cells was ~30% of wild-type mice (Fig. 5A). Analysis of lung cells using CD11c/Siglec F and light scatter/autofluorescence as markers of alveolar macrophages revealed >80% reduction in the frequency of this population in C/EBPβ$^{-/-}$ animals (Fig. 5B). Like peritoneal macrophages, C/EBPβ is highly expressed by alveolar macrophages (30), indicating that peritoneal and lung macrophages share C/EBPβ-dependent pathways of differentiation and/or survival. Notably, frequencies of CD11c^{-}Siglec F^{+} eosinophils in the lungs (and all tissues outside of the peritoneal cavity) were comparable in WT and KO animals (Fig. 5B). Unlike in the peritoneal cavity, the shortage of lung macrophages in C/EBPβ$^{-/-}$ mice was not associated with local eosinophilia.

Some tissue macrophages do not express the F4/80 antigen. In addition to F4/80^{+} red pulp macrophages (13), the spleen also contains F4/80^{-}MOMA-1^{+} metallophilic macrophages and F4/80^{-}SIGN-R1^{+} marginal zone macrophages that line the inner and outer border, respectively, of the marginal zone (40, 41). There were no differences in the distributions of splenic macrophage populations of C/EBPβ sufficient or -deficient mice (Supplemental Fig. 4A). Similarly, histological analyses did not reveal discernible changes in the F4/80^{+} or MOMA-1^{+} macrophage networks of the mesenteric lymph node (Supplemental Fig. 4B). C/EBPβ plays a tissue-restricted role for peritoneal and lung macrophages.

SPM are precursors for LPM

The abundance of SPM-like and F4/80^{int} macrophages but dearth of LPM in C/EBPβ KO mice (Fig. 3 and 4) suggested an ontogenic relationship between SPM and LPM, and a differentiative block in the absence of C/EBPβ. When C/EBPβ$^{+/+}$ SPM from GFP^{+} mice (42) were adoptively transferred into the peritoneal cavities of C/EBPβ$^{-/-}$ mice, the frequency of F4/80^{low} donor cells gradually decreased while the frequency of F4/80^{hi} LPM-like cells concomitantly increased; by day 8, over 85% of GFP^{+} cells were F4/80^{hi} and most

of these cells were MHCII^{low}CD93^{+}, identifying them as LPM (Fig. 6A, B). C/EBPβ is required intrinsically for SPM differentiation into LPM.

When SPM were transferred into C/EBPβ$^{+/+}$ or C/EBPβ$^{+/-}$ mice, however, only 20–40% of transferred cells were recovered as F4/80^{hi} cells (Fig. 6A). Moreover, <30% of the F4/80^{hi} donor cells bore the LPM phenotype of MHCII^{low}CD93^{+} and the majority still expressed MHCII, a characteristic of SPM, even 8 days after transfer (Fig. 6A). The efficient generation of LPM from transferred SPM in C/EBPβ KO, but not wild-type, hosts suggests a difference in the peritoneal microenvironment, perhaps relating to the presence or absence of endogenous LPM.

Resident peritoneal macrophages are reported to proliferate as a means of self-replenishment (20). Since LPM are missing in C/EBPβ$^{-/-}$ mice (Fig. 3), the appearance of LPM in C/EBPβ$^{-/-}$ mice after SPM transfer might represent proliferation of LPM contaminants in the adoptive transfer and not differentiation from SPM. Therefore, we transferred GFP^{+} LPM *i.p.* into C/EBPβ KO and control mice; if LPM proliferate in C/EBPβ$^{-/-}$ recipients, then we expected to recover more GFP^{+} LPM from C/EBPβ$^{-/-}$ hosts than from C/EBPβ^{+} hosts. Transferred LPM retained the LPM phenotype, even in C/EBPβ$^{-/-}$ hosts (Fig. 6C). However, the numbers of donor LPM recovered from C/EBPβ-sufficient and -deficient hosts were similar, even 30 days post-transfer (Fig. 6D). The equal recovery of donor LPM from KO and wild-type hosts excludes the possibility of expansion by LPM contaminants in adoptive transfer experiments.

Discussion

In this study, we reveal a crucial role for the C/EBPβ transcription factor in LPM generation. Adoptively transferred SPM efficiently differentiate into LPM in C/EBPβ$^{-/-}$ hosts, which lack endogenous LPM, but rarely generate LPM in wild-type hosts (Fig. 6). We conclude that SPM are targets of demand-driven differentiation signals that maintain macrophage homeostasis in the peritoneal cavity. Our findings uncover a novel, tissue-selective role for C/EBPβ in the generation of peritoneal and lung macrophages and may provide insight into a general mechanism that sustains macrophage populations in tissues.

The heterogeneity of macrophages in different tissues implies specific developmental pathways to control resident phagocyte differentiation. For example, mice deficient for the transcription factor Spi-C specifically lack splenic red pulp macrophages (13), a population that is intact in C/EBPβ$^{-/-}$ mice (Fig. 5); reciprocally, C/EBPβ$^{-/-}$ mice lack LPM, yet peritoneal macrophages are normal in Spi-C$^{-/-}$ mice (13). C/EBPβ and Spi-C, therefore, must represent two independent pathways of tissue macrophage generation. Given that liver macrophage, marginal zone macrophage, and metallophilic macrophage populations are intact in both C/EBPβ$^{-/-}$ and Spi-C$^{-/-}$ mice, these populations must be products of other differentiation pathways.

C/EBPβ has well-characterized roles in monocyte/macrophage responses to inflammation and stress (43). Moreover, C/EBPβ has been implicated in the polarization and/or function of myeloid cells exhibiting immunosuppressive properties, including myeloid-derived suppressor cells (44) and M2 macrophages (45). While these reports define the importance of C/EBPβ in the generation and/or function of myeloid cells during pernicious conditions, our study reveals novel roles for C/EBPβ in the production of macrophage compartments in unperturbed tissue. C/EBPβ is expressed by macrophages in several tissues but is distinctively elevated in LPM and alveolar macrophages (30). The selective sensitivity of LPM and alveolar macrophages to C/EBPβ deficiency (Fig. 5) may reflect shared

requirements for C/EBPβ gene targets for differentiation and/or survival in the peritoneal cavity and lung.

In general, three mechanisms have been implicated in the maintenance of tissue macrophage compartments: 1) proliferation *in situ* by resident macrophages (20); 2) recruitment and maturation of circulating precursors (46); and 3) mobilization of hematopoietic progenitors to the periphery and their subsequent proliferation and differentiation (47). Inflammation activates all of these mechanisms and most studies have relied on inflammatory stimuli or cytotoxic agents to study macrophage replenishment. It is unclear, however, which mechanism(s) is active for macrophage homeostasis. We show in a genetic model of macrophage deficiency with no evidence of inflammation, that the absence of a terminally-differentiated macrophage compartment (LPM) is sufficient to induce the maturation of the immediate precursor (SPM) (Fig. 6A). The absence of endogenous LPM in C/EBPβ$^{-/-}$ mice was not associated with proliferation by adoptively transferred LPM (Fig. 6D), suggesting SPM differentiation as an important, if not dominant, mechanism for macrophage replenishment. Thus, the C/EBPβ$^{-/-}$ mouse provides a potential tool to dissect mechanisms of macrophage homeostasis in the peritoneal cavity without the additional variables of inflammatory or cytotoxic treatments.

Whereas pathways of differentiation from hematopoietic progenitors to SPM and LPM were evident in BM reconstitution experiments (Fig. 2D), the ontogenic relationship between SPM and LPM was revealed only in C/EBPβ$^{-/-}$ mice (Fig. 6A, B), where LPM are scarce (Fig. 3C). Only in C/EBPβ$^{-/-}$ mice were we able to observe efficient generation of LPM from transferred SPM (Fig. 6A). The recovery of donor-derived LPM after SPM transfer into C/EBPβ KO, but not WT, hosts (Fig. 6A, B) indicates that SPM-to-LPM differentiation is mediated by an extrinsic signal that is scarce in control mice, but abundant in C/EBPβ$^{-/-}$ animals. The absence of endogenous LPM in C/EBPβ$^{-/-}$ mice may increase the availability of differentiation factors that act on transferred SPM. Alternatively, LPM in C/EBPβ-sufficient hosts may directly inhibit the maturation of transferred SPM. Precursor inhibition by cellular progeny is the hallmark of a process controlled by a demand-driven mechanism.

The notion that a demand-driven process directs the differentiation of transferred SPM in C/EBPβ$^{-/-}$ hosts is consistent with observations that adoptively transferred monocytes fail to generate lung macrophages unless endogenous tissue macrophages are first depleted (46). Our observations suggest that circulating CX_3CR1^+ precursors (likely monocytes) continuously seed the peritoneum to generate SPM. In steady-state conditions, SPM reside in tissue for only a few days before dying or leaving the peritoneal cavity (Fig. 2B). However, if LPM numbers decrease, as a result of inflammation or ablation via chemical or radioactive treatments, SPM readily mature into LPM. A reduction in LPM density may promote the recruitment of circulating precursors to increase the pool of precursors that differentiate into SPM and then LPM. Since SPM fail to form LPM in the absence of C/EBPβ we postulate that demand-driven signals of recruitment and differentiation are constitutively active in C/EBPβ$^{-/-}$ mice, resulting in an accumulation of SPM and undeveloped LPM. This hypothesis is consistent with the recent findings of Yona *et al.*(5), who observed monocyte-derived cells in the LPM compartment 8 weeks after *i.p.* injection of thioglycollate.

Although macrophages are generally thought to arise from circulating monocytes (1), recent studies indicate that many tissue macrophage compartments arise from yolk sac-derived precursors and persist into adulthood independent of hematopoiesis [reviewed in (48)]. Schulz *et al.* (4) found that, in general, F4/80 expression by tissue macrophages correlated with yolk sac (F4/80^{hi}) *vs.* hematopoietic (F4/80^{low}) descent, although the origins of peritoneal macrophages were not addressed in that study. Our BrdU uptake and lineage-

tracking studies (Fig. 2) support the hypothesis that F4/80^{hi} LPM are long-lived and require little hematopoietic input for steady-state maintenance (5, 21, 22) whereas F4/80^{low} SPM are short-lived products of hematopoiesis. However, in adoptive transfer experiments, we observed that a small percentage (<10%) of SPM transferred into wild-type mice acquired the F4/80^{hi}MHCII^{low}CD93^{+} phenotype of LPM (Fig. 6A), suggesting some degree of LPM generation from SPM in steady-state conditions. Our findings do not eliminate the possibility that LPM originate from yolk sac precursors; if they do, then observations of LPM phenotype cells in bone marrow chimeras (Fig. 2D) and SPM adoptive transfer experiments (Fig. 6A) indicate a pathway in which a yolk sac-derived macrophage compartment can be replaced by products of hematopoiesis. Demand-driven processes of differentiation from hematopoietic precursors may represent a general mechanism for the replacement of tissue macrophages of yolk sac origin.

Our analysis of peritoneal leukocytes extends previous observations of functional heterogeneity among macrophage and DC populations in the peritoneal cavity (10, 49). Peritoneal DC, SPM, and LPM were distinct in their capacities to phagocytose apoptotic thymocytes (LPM > SPM >> DC; Fig. 1C). DC, SPM, and LPM also differed in cytokine responses to LPS (Fig. 1B). Some of our observations are consistent with those of Dioszeghy *et al.*, who analyzed cytokines produced by F4/80^{hi}CD11b^{+} cells (LPM) and F4/80^{low}CD11b^{+} cells (likely representing a mixture of SPM and DC) from the peritoneal cavity (49). In both studies, F4/80^{hi} LPM produced more G-CSF and less IL-12p40 than F4/80^{low} SPM/DC. Whereas Dioszeghy *et al.* observed similar levels of KC and RANTES production by LPM and SPM/DC, we observed significantly more KC and less RANTES production by LPM (Supplemental Fig. 1). These differences may result from the use of different TLR ligands for *ex vivo* stimulation.

C/EBPβ is important for macrophages to express genes associated with alternative activation (45), a polarization state driven by Th2 cytokines. However, both C/EBPβ$^{-/-}$ and LysM$^{Cre/WT}$C/EBPβ$^{fl/fl}$ mice exhibited peritoneal eosinophilia (Supplemental Fig. 3B), a common consequence of a Th2-cytokine immune response. Serum concentrations of the Th2 cytokines IL-4, IL-5, and IL-13, however, were comparable in control and C/EBPβ$^{-/-}$ mice (Supplemental Fig. 3F), and there was no evidence of increased eosinophil production in C/EBPβ KO mice (Supplemental Fig. 3D). We suspect that peritoneal eosinophilia associated with C/EBPβ deficiency is not due to constitutive Th2 activity, but results from the inability of C/EBPβ$^{-/-}$ mice to produce functional LPM. If LPM are the primary scavengers of the peritoneal cavity, then their absence might result in the local accumulation of eosinophils. On the other hand, the recent finding of eosinophil support for macrophage homeostasis in adipose tissue (50) raises the possibility of a similar role for eosinophils in the maintenance of peritoneal macrophages.

Supplementary Material

Refer to Web version on PubMed Central for supplementary material.

Acknowledgments

Cell sorting was performed in the Duke Human Vaccine Institute Research Flow Cytometry Shared Resource directed by Dr. John Whitesides. Multiplex cytokine measurements were performed in the Duke Human Vaccine Institute Immune Reconstitution & Biomarker Analysis Shared Resource Facility under the direction of Dr. Gregory D. Sempowski.

Grant support: This work was supported by NIH grants AI24335 and AI56363 (to G.K.). The Duke Human Vaccine Institute Immune Reconstitution & Biomarker Shared Resource Facility is supported in part by NIH grants P30-AI051445 and UC6-AI058607 (to G.D.S).

Abbreviations

BM	bone marrow
C/EBP	CCAAT/enhancer binding protein
DC	Dendritic Cell
FGFP	farnesylated enhanced green fluorescent protein
LPM	Large Peritoneal Macrophage
LysM	Lysozyme M
SPM	Small Peritoneal Macrophage

References

1. van Furth R, Cohn ZA, Hirsch JG, Humphrey JH, Spector WG, Langevoort HL. The mononuclear phagocyte system: a new classification of macrophages, monocytes, and their precursor cells. Bull World Health Organ. 1972; 46:845–852. [PubMed: 4538544]
2. Gordon S, Taylor PR. Monocyte and macrophage heterogeneity. Nat Rev Immunol. 2005; 5:953–964. [PubMed: 16322748]
3. Geissmann F, Manz MG, Jung S, Sieweke MH, Merad M, Ley K. Development of monocytes, macrophages, and dendritic cells. Science. 2010; 327:656–661. [PubMed: 20133564]
4. Schulz C, Gomez Perdiguero E, Chorro L, Szabo-Rogers H, Cagnard N, Kierdorf K, Prinz M, Wu B, Jacobsen SE, Pollard JW, Frampton J, Liu KJ, Geissmann F. A lineage of myeloid cells independent of Myb and hematopoietic stem cells. Science. 2012; 336:86–90. [PubMed: 22442384]
5. Yona S, Kim KW, Wolf Y, Mildner A, Varol D, Breker M, Strauss-Ayali D, Viukov S, Guilliams M, Misharin A, Hume DA, Perlman H, Malissen B, Zelzer E, Jung S. Fate Mapping Reveals Origins and Dynamics of Monocytes and Tissue Macrophages under Homeostasis. Immunity. 2013; 38:79–91. [PubMed: 23273845]
6. Wong K, Valdez PA, Tan C, Yeh S, Hongo JA, Ouyang W. Phosphatidylserine receptor Tim-4 is essential for the maintenance of the homeostatic state of resident peritoneal macrophages. Proc Natl Acad Sci U S A. 2010; 107:8712–8717. [PubMed: 20421466]
7. Kolaczkowska E, Lelito M, Kozakiewicz E, van Rooijen N, Plytycz B, Arnold B. Resident peritoneal leukocytes are important sources of MMP-9 during zymosan peritonitis: superior contribution of macrophages over mast cells. Immunol Lett. 2007; 113:99–106. [PubMed: 17826846]
8. Leendertse M, Willems RJ, Giebelen IA, Roelofs JJ, van Rooijen N, Bonten MJ, van der Poll T. Peritoneal macrophages are important for the early containment of Enterococcus faecium peritonitis in mice. Innate Immun. 2009; 15:3–12. [PubMed: 19201820]
9. Cailhier JF, Partolina M, Vuthoori S, Wu S, Ko K, Watson S, Savill J, Hughes J, Lang RA. Conditional macrophage ablation demonstrates that resident macrophages initiate acute peritoneal inflammation. J Immunol. 2005; 174:2336–2342. [PubMed: 15699170]
10. Ghosn EE, Cassado AA, Govoni GR, Fukuhara T, Yang Y, Monack DM, Bortoluci KR, Almeida SR, Herzenberg LA. Two physically, functionally, and developmentally distinct peritoneal macrophage subsets. Proc Natl Acad Sci U S A. 2010; 107:2568–2573. [PubMed: 20133793]
11. Heath V, Suh HC, Holman M, Renn K, Gooya JM, Parkin S, Klarmann KD, Ortiz M, Johnson P, Keller J. C/EBPalpha deficiency results in hyperproliferation of hematopoietic progenitor cells and disrupts macrophage development in vitro and in vivo. Blood. 2004; 104:1639–1647. [PubMed: 15073037]
12. McKercher SR, Torbett BE, Anderson KL, Henkel GW, Vestal DJ, Baribault H, Klemsz M, Feeney AJ, Wu GE, Paige CJ, Maki RA. Targeted disruption of the PU.1 gene results in multiple hematopoietic abnormalities. EMBO J. 1996; 15:5647–5658. [PubMed: 8896458]

13. Kohyama M, Ise W, Edelson BT, Wilker PR, Hildner K, Mejia C, Frazier WA, Murphy TL, Murphy KM. Role for Spi-C in the development of red pulp macrophages and splenic iron homeostasis. Nature. 2009; 457:318–321. [PubMed: 19037245]
14. Robinson GW, Johnson PF, Hennighausen L, Sterneck E. The C/EBPbeta transcription factor regulates epithelial cell proliferation and differentiation in the mammary gland. Genes Dev. 1998; 12:1907–1916. [PubMed: 9637691]
15. Gong S, Doughty M, Harbaugh CR, Cummins A, Hatten ME, Heintz N, Gerfen CR. Targeting Cre recombinase to specific neuron populations with bacterial artificial chromosome constructs. J Neurosci. 2007; 27:9817–9823. [PubMed: 17855595]
16. Sterneck E, Zhu S, Ramirez A, Jorcano JL, Smart RC. Conditional ablation of C/EBP beta demonstrates its keratinocyte-specific requirement for cell survival and mouse skin tumorigenesis. Oncogene. 2006; 25:1272–1276. [PubMed: 16205634]
17. Lu Y, Futtner C, Rock JR, Xu X, Whitworth W, Hogan BL, Onaitis MW. Evidence that SOX2 overexpression is oncogenic in the lung. PLoS One. 2010; 5:e11022. [PubMed: 20548776]
18. Miksa M, Komura H, Wu R, Shah KG, Wang P. A novel method to determine the engulfment of apoptotic cells by macrophages using pHrodo succinimidyl ester. J Immunol Methods. 2009; 342:71–77. [PubMed: 19135446]
19. Liu K, Nussenzweig MC. Origin and development of dendritic cells. Immunol Rev. 2010; 234:45–54. [PubMed: 20193011]
20. Davies LC, Rosas M, Smith PJ, Fraser DJ, Jones SA, Taylor PR. A quantifiable proliferative burst of tissue macrophages restores homeostatic macrophage populations after acute inflammation. Eur J Immunol. 2011; 41:2155–2164. [PubMed: 21710478]
21. Ansel KM, Harris RB, Cyster JG. CXCL13 is required for B1 cell homing, natural antibody production, and body cavity immunity. Immunity. 2002; 16:67–76. [PubMed: 11825566]
22. Melnicoff MJ, Horan PK, Breslin EW, Morahan PS. Maintenance of peritoneal macrophages in the steady state. J Leukoc Biol. 1988; 44:367–375. [PubMed: 2460572]
23. Auffray C, Sieweke MH, Geissmann F. Blood monocytes: development, heterogeneity, and relationship with dendritic cells. Annu Rev Immunol. 2009; 27:669–692. [PubMed: 19132917]
24. Natsuka S, Akira S, Nishio Y, Hashimoto S, Sugita T, Isshiki H, Kishimoto T. Macrophage differentiation-specific expression of NF-IL6, a transcription factor for interleukin-6. Blood. 1992; 79:460–466. [PubMed: 1730090]
25. Liebermann DA, Hoffman B. Differentiation primary response genes and proto-oncogenes as positive and negative regulators of terminal hematopoietic cell differentiation. Stem Cells. 1994; 12:352–369. [PubMed: 7951003]
26. Krausgruber T, Blazek K, Smallie T, Alzabin S, Lockstone H, Sahgal N, Hussell T, Feldmann M, Udalova IA. IRF5 promotes inflammatory macrophage polarization and TH1-TH17 responses. Nat Immunol. 2011; 12:231–238. [PubMed: 21240265]
27. Aziz A, Soucie E, Sarrazin S, Sieweke MH. MafB/c-Maf deficiency enables self-renewal of differentiated functional macrophages. Science. 2009; 326:867–871. [PubMed: 19892988]
28. Steingrimsson E, Tessarollo L, Pathak B, Hou L, Arnheiter H, Copeland NG, Jenkins NA. Mitf and Tfe3, two members of the Mitf-Tfe family of bHLH-Zip transcription factors, have important but functionally redundant roles in osteoclast development. Proc Natl Acad Sci U S A. 2002; 99:4477–4482. [PubMed: 11930005]
29. Marziali G, Perrotti E, Ilari R, Testa U, Coccia EM, Battistini A. Transcriptional regulation of the ferritin heavy-chain gene: the activity of the CCAAT binding factor NF-Y is modulated in heme-treated Friend leukemia cells and during monocyte-to-macrophage differentiation. Mol Cell Biol. 1997; 17:1387–1395. [PubMed: 9032265]
30. Gautier EL, Shay T, Miller J, Greter M, Jakubzick C, Ivanov S, Helft J, Chow A, Elpek KG, Gordonov S, Mazloom AR, Ma'ayan A, Chua WJ, Hansen TH, Turley SJ, Merad M, Randolph GJ. Gene-expression profiles and transcriptional regulatory pathways that underlie the identity and diversity of mouse tissue macrophages. Nat Immunol. 2012; 13:1118–1128. [PubMed: 23023392]
31. Sterneck E, Tessarollo L, Johnson PF. An essential role for C/EBPbeta in female reproduction. Genes Dev. 1997; 11:2153–2162. [PubMed: 9303532]

32. Tanaka T, Akira S, Yoshida K, Umemoto M, Yoneda Y, Shirafuji N, Fujiwara H, Suematsu S, Yoshida N, Kishimoto T. Targeted disruption of the NF-IL6 gene discloses its essential role in bacteria killing and tumor cytotoxicity by macrophages. Cell. 1995; 80:353–361. [PubMed: 7530603]
33. Yan C, Wu M, Cao J, Tang H, Zhu M, Johnson PF, Gao H. Critical role for CCAAT/enhancer-binding protein beta in immune complex-induced acute lung injury. J Immunol. 2012; 189:1480–1490. [PubMed: 22732594]
34. Screpanti I, Romani L, Musiani P, Modesti A, Fattori E, Lazzaro D, Sellitto C, Scarpa S, Bellavia D, Lattanzio G, et al. Lymphoproliferative disorder and imbalanced T-helper response in C/EBP beta-deficient mice. Embo J. 1995; 14:1932–1941. [PubMed: 7744000]
35. Gorgoni B, Maritano D, Marthyn P, Righi M, Poli V. C/EBP beta gene inactivation causes both impaired and enhanced gene expression and inverse regulation of IL-12 p40 and p35 mRNAs in macrophages. J Immunol. 2002; 168:4055–4062. [PubMed: 11937564]
36. Matsusaka T, Fujikawa K, Nishio Y, Mukaida N, Matsushima K, Kishimoto T, Akira S. Transcription factors NF-IL6 and NF-kappa B synergistically activate transcription of the inflammatory cytokines, interleukin 6 and interleukin 8. Proc Natl Acad Sci U S A. 1993; 90:10193–10197. [PubMed: 8234276]
37. Tanaka T, Yoshida N, Kishimoto T, Akira S. Defective adipocyte differentiation in mice lacking the C/EBPbeta and/or C/EBPdelta gene. EMBO J. 1997; 16:7432–7443. [PubMed: 9405372]
38. Clausen BE, Burkhardt C, Reith W, Renkawitz R, Forster I. Conditional gene targeting in macrophages and granulocytes using LysMcre mice. Transgenic Res. 1999; 8:265–277. [PubMed: 10621974]
39. Screpanti I, Musiani P, Bellavia D, Cappelletti M, Aiello FB, Maroder M, Frati L, Modesti A, Gulino A, Poli V. Inactivation of the IL-6 gene prevents development of multicentric Castleman's disease in C/EBP beta-deficient mice. J Exp Med. 1996; 184:1561–1566. [PubMed: 8879230]
40. Kraal G, Janse M. Marginal metallophilic cells of the mouse spleen identified by a monoclonal antibody. Immunology. 1986; 58:665–669. [PubMed: 3733156]
41. Dijkstra CD, Van Vliet E, Dopp EA, van der Lelij AA, Kraal G. Marginal zone macrophages identified by a monoclonal antibody: characterization of immuno- and enzyme-histochemical properties and functional capacities. Immunology. 1985; 55:23–30. [PubMed: 3888828]
42. Okabe M, Ikawa M, Kominami K, Nakanishi T, Nishimune Y. `Green mice' as a source of ubiquitous green cells. FEBS Lett. 1997; 407:313–319. [PubMed: 9175875]
43. Huber R, Pietsch D, Panterodt T, Brand K. Regulation of C/EBPbeta and resulting functions in cells of the monocytic lineage. Cell Signal. 2012; 24:1287–1296. [PubMed: 22374303]
44. Marigo I, Bosio E, Solito S, Mesa C, Fernandez A, Dolcetti L, Ugel S, Sonda N, Bicciato S, Falisi E, Calabrese F, Basso G, Zanovello P, Cozzi E, Mandruzzato S, Bronte V. Tumor-induced tolerance and immune suppression depend on the C/EBPbeta transcription factor. Immunity. 2010; 32:790–802. [PubMed: 20605485]
45. Ruffell D, Mourkioti F, Gambardella A, Kirstetter P, Lopez RG, Rosenthal N, Nerlov C. A CREB-C/EBPbeta cascade induces M2 macrophage-specific gene expression and promotes muscle injury repair. Proc Natl Acad Sci U S A. 2009; 106:17475–17480. [PubMed: 19805133]
46. Landsman L, Varol C, Jung S. Distinct differentiation potential of blood monocyte subsets in the lung. J Immunol. 2007; 178:2000–2007. [PubMed: 17277103]
47. Massberg S, Schaerli P, Knezevic-Maramica I, Kollnberger M, Tubo N, Moseman EA, Huff IV, Junt T, Wagers AJ, Mazo IB, von Andrian UH. Immunosurveillance by hematopoietic progenitor cells trafficking through blood, lymph, and peripheral tissues. Cell. 2007; 131:994–1008. [PubMed: 18045540]
48. Wynn TA, Chawla A, Pollard JW. Macrophage biology in development, homeostasis and disease. Nature. 2013; 496:445–455. [PubMed: 23619691]
49. Dioszeghy V, Rosas M, Maskrey BH, Colmont C, Topley N, Chaitidis P, Kuhn H, Jones SA, Taylor PR, O'Donnell VB. 12/15-Lipoxygenase regulates the inflammatory response to bacterial products in vivo. J Immunol. 2008; 181:6514–6524. [PubMed: 18941242]

50. Wu D, Molofsky AB, Liang HE, Ricardo-Gonzalez RR, Jouihan HA, Bando JK, Chawla A, Locksley RM. Eosinophils sustain adipose alternatively activated macrophages associated with glucose homeostasis. Science. 2011; 332:243–247. [PubMed: 21436399]

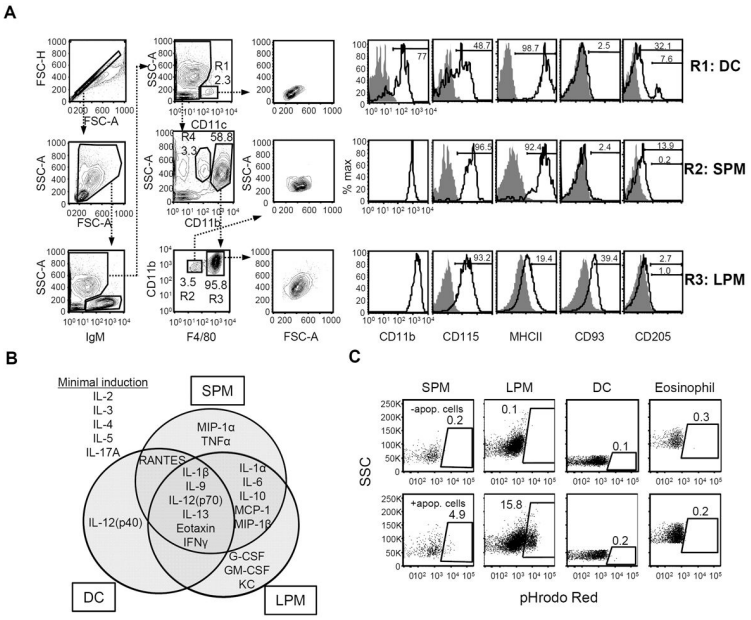

Figure 1. Effector functions of SPM and LPM

(A) Flow cytometric gating strategy to identify peritoneal DC (R1: IgM^{-}CD11c^{+}SSC^{low}), SPM (R2: IgM^{-}CD11c^{-}CD11b^{hi}F4/80^{low}), and LPM (R3: IgM^{-}CD11c^{-}CD11b^{hi}F4/80^{hi}) in peritoneal lavages of C57BL/6 mice. Cells in gate R4 (IgM^{-}CD11c^{-}CD11b^{int}SSC^{hi}) were identified as eosinophils. Forward- and side light scattering (FSC and SSC) properties and surface expression of CD11b, CD115, MHCII (I-A/I-E), CD93, and CD205 (open histograms) for each compartment is shown in histograms to the right. Gray histograms depict background staining by isotype-matched control antibodies. (B) Cytokine signatures of sorted peritoneal DC, SPM, and LPM following *in vitro* exposure to LPS. The concentrations of various cytokines in the supernatants were determined by multiplex bead array. Data are summarized here in a Venn diagram and detailed in Supplemental Figure 1. Data represent three independent experiments, n=3–7 samples per cell type. (C) Peritoneal cells were assessed for their ability to phagocytose apoptotic cells *in vivo*. pHrodo Red-labeled apoptotic thymocytes were injected *i.p.* and then peritoneal lavages were performed 1 hour later. Phagocytosis was measured as the frequency of pHrodo Red-labeled cells in the SPM, LPM, DC, and eosinophil compartments. The upper row shows representative dot plots of background fluorescence by cells of untreated mice, whereas the lower row depicts plots of gated cells from a mouse injected with labeled apoptotic cells. Data are representative of two individual experiments; n=4 mice.

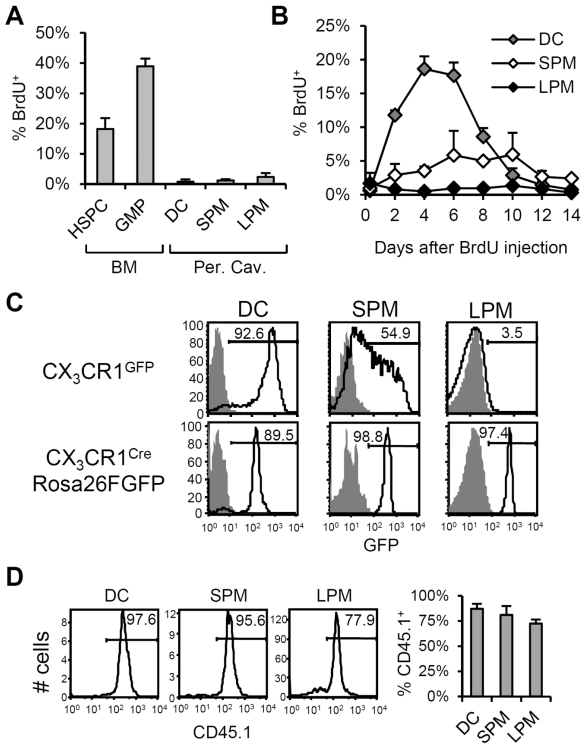

Figure 2. Origins and maintenance of peritoneal DC, SPM, and LPM

(A) To measure proliferation in peritoneal myeloid compartments, C57BL/6 mice were injected *i.p.* with BrdU. Three hours later, peritoneal DC, SPM, and LPM were analyzed for BrdU uptake. Bone marrow hematopoietic stem and progenitor cells (HSPC: $Lin^{-}c\text{-}Kit^{+}Sca\text{-}1^{+}$) and granulocyte/macrophage progenitors (GMP: $Lin^{-}c\text{-}Kit^{+}Sca\text{-}1^{-}CD34^{+}CD16/32^{+}$) were harvested as controls. The mean(±SD) frequency of $BrdU^{+}$ cells in each compartment is shown. (B) BrdU transit through peritoneal DC, SPM, and LPM compartments after a single BrdU pulse. The mean(±SD) frequencies of $BrdU^{+}$ cells in the DC (gray), SPM (white), and LPM (black) compartments at intervals after BrdU administration are shown. Data represent two independent experiments, n=2–4 mice per data point. (C) CX_3CR1 expression by peritoneal DC, SPM, and LPM. In the top row, GFP fluorescence by cells from $CX_3CR1^{GFP/wt}$ mice (open histogram) and C57BL/6 controls (shaded histogram) is shown. In the bottom row, GFP fluorescence by peritoneal DC, SPM, and LPM from $CX_3CR1^{Cre/wt}$Rosa26R-FGFP mice (open histogram) and control $CX_3CR1^{wt/wt}$Rosa26R-FGFP (shaded histogram) is shown. Histograms are representative of results in two independent experiments, n=3–4 mice per genotype. (D) Reconstitution of peritoneal DC, SPM, and LPM following irradiation and BM transfer. C57BL/6.CD45.1 BM cells were adoptively transferred into irradiated C57BL/6.CD45.2 hosts. Representative histograms show frequencies of donor-derived ($CD45.1^{+}$) cells in peritoneal DC, SPM, and LPM compartments 4–5 weeks after reconstitution. At right, the mean(±SD) frequencies of $CD45.1^{+}$ cells in each compartment are shown. Data represent two independent experiments, n=4 mice.

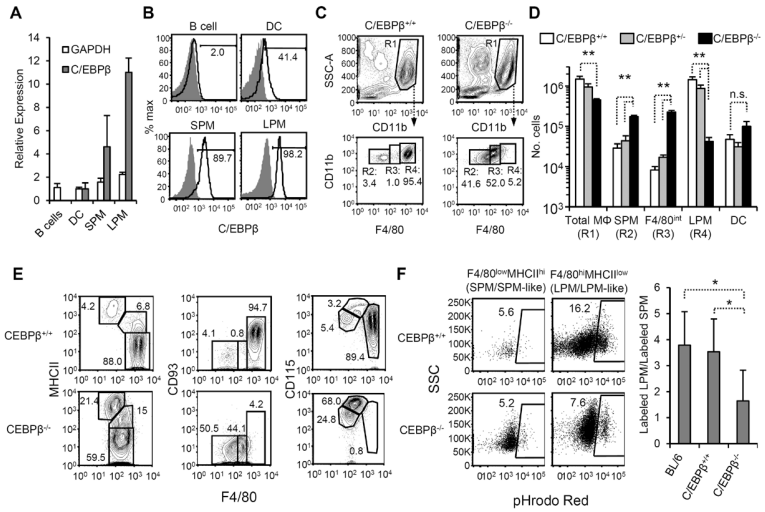

Figure 3. Effect of C/EBPβ deficiency on peritoneal macrophages

(A) Peritoneal B cells (IgM^+), peritoneal DC, SPM, and LPM were sorted (gated as in Fig. 1A) and analyzed for C/EBPβ, GAPDH, and β-actin transcripts by quantitative RT-PCR. We measured C/EBPβ and GAPDH transcription relative to β-actin and then normalized to the average value of the peritoneal DC compartment. Values represent the geometric mean (±GSD) from three individual sorts. (B) C/EBPβ protein in SPM, LPM, peritoneal DC, and B cells. Intracellular staining of peritoneal cells with anti-C/EBPβ (open histogram) or isotype control (gray histogram) is shown. Data are representative of 2 individual experiments, n=2. (C) Representative flow cytometric analyses of peritoneal macrophages in C/EBP$\beta^{+/+}$ and C/EBP$\beta^{-/-}$ mice. In the top row of dot plots, IgM^+ and $CD11c^+$ cells have been excluded as in Fig. 1A; $SSC^{hi}CD11b^{hi}$ cells are gated as total macrophages (R1: "Total MΦ"). F4/80 and CD11b expression by total macrophages of C/EBP$\beta^{+/+}$ and C/EBP$\beta^{-/-}$ mice are shown in the bottom row, and populations have been subdivided by F4/80 staining intensity (R2: "SPM", R3: "$F4/80^{int}$", and R4: "LPM"). (D) The mean(±SD) numbers of Total MΦ, $F4/80^{low}$ SPM, $F4/80^{int}$ macrophages, and $F4/80^{hi}$ LPM from C/EBP$\beta^{+/+}$(open bars), C/EBP$\beta^{+/-}$ (gray bars), and C/EBP$\beta^{-/-}$ (black bars) are shown. Data represent 9 independent experiments, n=6–8 mice per genotype. * P≤0.05, ** P≤0.01 *vs.* C/EBP$\beta^{+/+}$ mice. n.s., not significant. (E) Phenotypic analysis of total macrophages (R1) macrophages from C/EBP$\beta^{+/+}$ (top row) and C/EBP$\beta^{-/-}$ (bottom row) mice. In all dot plots, F4/80 is shown on the x-axis and MHCII, CD93, and CD115 on the y-axes. Data are representative of 2–3 experiments, n≥3 mice per antibody panel. (F) The phagocytic capacity of C/EBP$\beta^{+/+}$ (top row) and C/EBP$\beta^{-/-}$ (bottom row) macrophages was assessed following *i.p.* injection of pHrodo Red-labeled apoptotic thymocytes. Macrophages were gated based on F4/80 and MHCII expression as in the left panel of Fig. 3E. SPM and SPM-like macrophages were gated as $F4/80^{low}MHCII^{hi}$ SPM; LPM and LPM-like macrophages were gated as $F4/80^{hi}MHCII^{low}$ (C/EBP$\beta^{+/+}$ mice) and $F4/80^{int}MHCII^{low}$ (C/EBP$\beta^{-/-}$ mice) cells, respectively. The right panel shows the ratio (geometric mean±GSD) of labeled $F4/80^{int/hi}MHCII^{low}$ macrophages to $F4/80^{low}MHCII^{hi}$ macrophages in C57BL/6, C/EBP$\beta^{+/+}$ littermates, and C/EBP$\beta^{-/-}$ mice. Flow plots are representative of 2 individual experiments, n=2–4 mice per genotype. * P≤0.05.

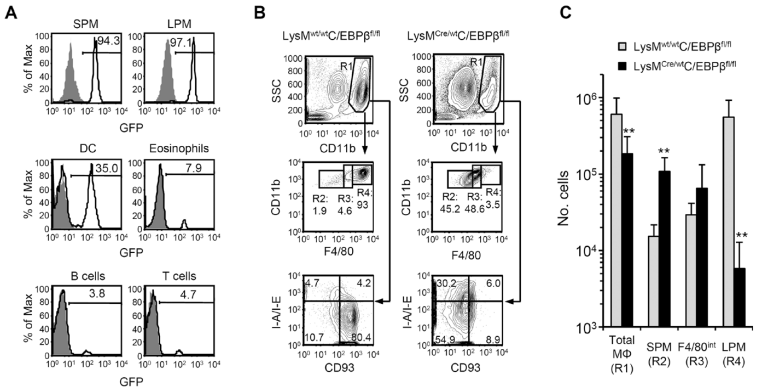

Figure 4. Abnormal distribution of peritoneal macrophage populations in LysM$^{Cre/WT}$C/EBPβ$^{fl/fl}$ mice

(A) FGFP expression in SPM, LPM, DC, CD11b^{int}SSC^{hi} eosinophils, IgM^{+} B cells, and TCRβ^{+} T cells in peritoneal lavages of LysM$^{Cre/WT}$Rosa26R-FGFP mice (open histograms) and control LysM$^{WT/WT}$Rosa26R-FGFP mice (gray histograms). (B) Representative flow cytometric analyses of peritoneal macrophages in LysM$^{wt/wt}$C/EBPβ$^{fl/fl}$ and LysM$^{Cre/wt}$C/EBPβ$^{fl/fl}$ mice. In the top row of dot plots, cells expressing IgM or CD11c have been excluded and SSC^{hi}CD11b^{hi} cells gated as total macrophages (R1: “Total MΦ”). F4/80 and CD11b expression by total macrophages of C/EBPβ$^{+/+}$ and C/EBPβ$^{-/-}$ mice is shown in the middle row, and populations have been subdivided by F4/80 staining intensity (R2: “SPM”, R3: “F4/80^{int}”, and R4: “LPM”); CD93 and MHCII expression by total macrophages is shown in the lowest row. (C) The mean(±SD) numbers of Total MΦ, SPM, F4/80^{int} macrophages, and LPM from LysM$^{wt/wt}$C/EBPβ$^{fl/fl}$ mice (gray bars) and LysM$^{Cre/wt}$C/EBPβ$^{fl/fl}$ mice (black bars) are shown. Data represent two independent experiments, n=8–9 mice per genotype. ** P≤0.01.

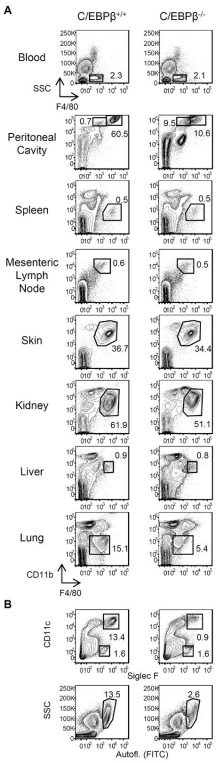

Figure 5. Survey of tissue macrophages in C/EBPβ$^{-/-}$ mice

(A) Single-cell suspensions of blood, peritoneal cavity, spleen, mesenteric lymph nodes, skin (ear), kidney, liver, and lungs of C/EBPβ$^{+/+}$ and C/EBPβ$^{-/-}$ mice were stained for CD45, F4/80, and CD11b. Viable CD45^{+} cells were gated for analysis of F4/80^{+} macrophage/monocyte populations. (B) Viable CD45^{+} lung cells from C/EBPβ$^{+/+}$ and C/EBPβ$^{-/-}$ mice were analyzed for the presence of alveolar macrophages using Siglec F and CD11c (top row), and side-scatter (SSC) and autofluorescence (bottom row). Flow plots are representative of 2 individual experiments, n=3 mice per genotype.

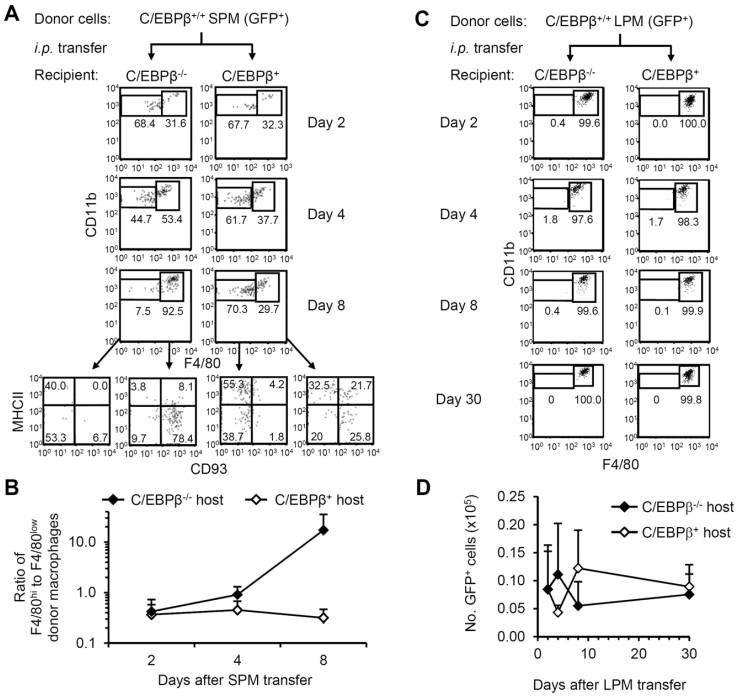

Figure 6. SPM efficiently differentiate into LPM when adoptively transferred into C/EBPβ-deficient, but not -sufficient, hosts

(A) C/EBP$\beta^{+/+}$GFP$^{+/+}$ SPM were isolated by cell sorting and injected *i.p.* into C/EBPβ-sufficient or -deficient hosts. Representative FACS plots of F4/80 and CD11b staining of GFP^{+}IgM^{-}CD11c^{-} peritoneal cells recovered on days 2, 4, and 8 after transfer are shown. For day 8, MHCII and CD93 staining is shown for F4/80^{low} and F4/80^{hi} donor cells. (B) The ratio of F4/80^{hi} cells to F4/80^{low} cells was calculated in each mouse receiving GFP^{+} SPM. The geometric mean(±GSD) ratio of F4/80^{hi} cells to F4/80^{low} cells at each time point after transfer is shown. Data represent 4 independent experiments; n=2–4 mice per data point. (C) LPM from C/EBP$\beta^{+/+}$GFP$^{+/+}$ mice were isolated by cell sorting and injected *i.p.* into C/EBPβ-sufficient or -deficient hosts. Representative FACS plots of F4/80 and CD11b staining of GFP^{+}IgM^{-}CD11c^{-} cells on days 2, 4, 8, and 30 after transfer are shown. (D) The mean(±SD) numbers of GFP^{+} cells recovered in peritoneal lavages after adoptive transfer of C/EBP$\beta^{+/+}$GFP$^{+/+}$ LPM into C/EBPβ-sufficient (C/EBP$\beta^{+/+}$ or C/EBP$\beta^{+/-}$) or -deficient hosts are shown. Data represent 5 independent experiments; n=2–4 mice per data point.